International Journal of Engineering Research and Science & Technology

www.ijerst.org

ISSN : 2319-5991

Vol. 21 No. 3 (1) 2025



ijerst.editor@gmail.com

editor@ijerst.com

International Journal of Engineering Research and Science & Technology

ISSN 2319-5991 www.ijerst.com
Vol. 21, No. 3(1), 2025
© 2025 IJERST. All Rights Reserved

Research Paper

COORDINATED CONTROL OF A WIND TURBINE–DRIVEN DFIG SYSTEM WITH SOLAR PV–BATTERY STORAGE FOR REMOTE AREA DISTRIBUTED GENERATION

Thota Sathvika[1] DR. K. Ranjith Kumar[2]

[1]M. Tech Student, Department of Electrical and Electronics Engineering, Vaagdevi College of Engineering, Khammam - Warangal Hwy, Road, Bollikunta, Telangana 506005

[2]Associate Professor, Department of Electrical and Electronics Engineering, Vaagdevi College of Engineering, Khammam - Warangal Hwy, Road, Bollikunta, Telangana 506005

Abstract *This article presents a synchronizing control for wind turbine (WT) driven doubly fed induction generator (DFIG) system with DG (Diesel Generator) in a remote area consisting of solar photovoltaic (PV) array and the battery energy storage. The DFIG is operated with two voltage source converters (VSCs) namely VSC on rotor side (VSCR) and VSC on load side (VSCL) by sharing common DC link with a battery. Moreover, the solar PV array is connected to the DC link through a boost converter, which is used to acquire peak power from the PV array. The microgrid is designed with minimum power converters with enhanced reliability and reduced intermittency especially for islands. Moreover, two controls are presented for successful and smooth operation of microgrid. An additional frequency loop is added in the control of VSCR for minimizing the power fluctuations and for smooth connection of DG to DFIG-solar-battery based isolated microgrid with static transfer switch. Moreover, the VSCR control is framed to build the rated voltage at the DFIG stator with control over ON/OFF operation of VSCR. It is also designed to harness the maximum power from wind. The control of VSCL is framed to regulate the DG power to operate it in optimal fuel consumption zone whenever it is synchronized. Simulations are performed at steady and varying wind speeds, varying PV insolation and at unbalanced connected loads.*

Received: 08-07-2025 Accepted: 22-07-2025 Published: 11-08-2025

1. Introduction

Even in the present scenario, there are locations with no grid availability. In such locations, diesel generation plays key role in feeding the base load requirements though it involves operational expenditure due to its fuel. However, the main benefit is its dispatchable operation. This is why in many islands, diesel generators (DGs) are used as a source of power. However, it is essential to minimize the pollution otherwise, it leads to global warming and many other harmful effects. Currently, the world is focused on harnessing the energy from renewable sources like wind and solar. It is because, they are non-pollutants and ample in the nature. The integration of DG with wind and solar, reduces its operational fuel cost. Moreover, its combination improves the reliability. The doubly fed induction generator (DFIG) is used widely at wind power sites because of its merits such as fractional rated converters, favourable for variable speeds with MPPT (Maximum Power Point Tracking) operation, simple manufacturing and maintenance.

It is also apparent that there are issues of microgrids with distributed sources. The impacts of distributed generation penetration have been discussed, the authors have discussed the impacts of high penetration of renewables based distributed

generation on the tap operation of under-load tap changer in the power network. Moreover, various challenges have been discussed especially the interaction between the voltage control equipment and the distributed generation. the authors have proposed an optimized fast frequency controller for DFIG based wind turbines to improve the frequency response under the high penetration of renewables such as wind. Moreover, case studies have been performed to prove the effectiveness of fast frequency controller. In other side, as most of the wind farms uses DFIG, there has been significant research going all over the globe especially in control advancements, the authors have developed a rooted tree optimization algorithm for wind-DFIG systems, which is based on adaptive backstepping control. Moreover, it has been applied to both converters of DFIG for achieving the insensitive system to parametric variations.

The authors have demonstrated the wind-DFIG system with a sensorless control. The rotor speed has been estimated from the second order generalized integrator based adaptive algorithm and rotor position correction. the authors have presented an enhanced estimation of rotor position for DFIG based wind turbines. Moreover, it does not require the initial position of rotor. the authors have proposed a new frequency control technique for wind-DFIG systems by considering the wake effect.

Moreover, the control has been developed with the incorporation of primary frequency and virtual inertia controls. the authors have proposed an adaptive sliding mode control for voltage source converter on load side (VSCL) to regulate the stability of wind-diesel power system. However, it lacks the synchronization control for smooth connection of DFIG system to the DG. the authors have demonstrated a hybrid system based on wind and diesel with a battery for the optimal fuel operation. However, it requires higher battery rating because of only two power sources. Moreover, it has more power fluctuations because it does not have frequency loop. In , the authors have presented a model-free predictive current control for the synchronization of DFIG to the grid. However, wind fluctuations have not been taken in to account for the design of control algorithm. Moreover, the grid side VSC control has not been discussed. the authors have demonstrated a microgrid based on wind turbine driven synchronous reluctance generator, solar photovoltaic (PV) array and a battery .Moreover, seamless transition controls have been presented for smooth interaction to the grid based on its availability. the authors have presented an overview of grid forming converters and their various control schemes. Moreover, various controls of grid synchronization have been discussed. the authors have presented a microgrid based on wind-DFIG, solar PV array and the battery, which is suitable to operate in islanding and grid connected modes. Moreover, seamless transition controls for both converters of DFIG have been discussed. Metal. It have proposed a robust load frequency control for wind-diesel based isolated microgrid. Moreover, the control has been incorporated with dual loop compensations for suppressing the variations in frequency, which is common with renewables penetration. However, the results have not been discussed during DG connection. have presented the control for DFIG with inertial response loop to balance the frequency fluctuations at grid side in a diesel-wind system. However, both DFIG and DG have been connected to grid directly and, moreover, coordination control between DFIG and DG, have not been analyzed. have discussed the power management techniques for a microgrid with wind-diesel-hydrogen based generation. Moreover, the controls have been framed to extract maximum power from wind generator during uncertainty of generation. However, the system has not been tested experimentally Demonstrated.

The voltage-source converter is widely used as an interface for the renewable energy systems before they are linked to the grid like in the photovoltaic and wind power system cases, with its advantages in fully control of dc-link voltage, active and reactive power, as well as power factor A grid filter is normally introduced to avoid the pulse width modulation carrier and side-band voltage harmonics coupling to the grid that can disturb other sensitive loads or equipment. For the megawatt-level wind power converter, due to the quite low switching frequency of the power switching devices (usually several kilohertz), a simple filter inductor consequently becomes bulky, expensive, and it may also bring poorer dynamics into the system.

In order to fulfill the modern grid codes], the wind turbine system is currently required to behave

more like a traditional power source (e.g., synchronous generator), which implies that the wind turbine system should have the capability of reactive power support. Due to the doubly fed mechanism of the doubly fed induction generator (DFIG)-based wind turbine system, the reactive power can be supported either by the grid-side converter (GSC) or the rotor-side converter (RSC). If the reactive power is provided by the GSC, in the case of the constant dc-link voltage, the modulation index is closely related to the filter inductance, and it will increase very fast to over modulation, especially when overexcited (OE) reactive power is needed.

There are two ways to deal with this issue—increase the dc-link voltage, which gives higher switching loss and power rating, or design an optimized grid filter. Besides, if a small amount of reactive power is demanded by the transmission system operator, it is also of interest to compare the loss of the whole DFIG system, as the reactive power supported by the GSC only affects the loss of the GSC, while the reactive provided by the RSC not only influences the loss of the RSC, but also the loss of the generator itself. Then, the annual energy loss of the wind turbine system and cost of the reactive power can be calculated based on the annual wind profile at different compensation schemes.

2. System configuration and operating principle

The standalone wind-diesel system for water treatment application and moreover, a permanent magnet synchronous generator has been used for wind energy extraction. However, the controls have been designed for the continuous operation of DG even at higher wind generation. Khalil et al. [20] have presented an artificial rabbits optimization control flow for the load frequency control in an isolated microgrid. The algorithm basically tunes the conventional controller constants automatically with changes in the load frequency thereby it provides the sufficient inertial response. However, experimental performance has not been discussed. Furthermore, in [21], the authors have discussed the turbulent flow water-based optimization technique for optimal sizing of different sources of power generation such as wind, solar, DG and battery. However, the microgrid performance for seamless connection of wind and DG, has not been analysed. Moreover, Mohammad-Alikhani et al. [22] have demonstrated the multi objective optimization control for both capacity and components selection in a microgrid with sources namely wind, solar, DG and battery etc.

However, the power control for coordination of different sources has not been analysed. have presented a decentralized controller for the coupled wind turbine-diesel engine generator based isolated system with both frequency and active power control. However, the experimental results have not been analyzed. Moreover, in [24], the authors have demonstrated an optimal economic dispatch of different sources such as wind, solar, DG and battery in a microgrid with a mathematical approach. However, the point of connection and seamless operation of different sources have not been discussed. In [25], the authors have presented a power management strategy for wind-diesel-solar microgrid based on adaptive fuzzy logic control. However, in its configuration, the DFIG system is connected to the DG at point of common coupling (PCC) without static switch. Moreover, its coordinated control has not been considered the variations in wind for the smooth connection.

This study focuses on synchronizing control of wind turbine (WT) driven DFIG to the DG in an isolated microgrid involving solar PV array and battery energy storage (BES). The contributions of this work, are as follows.

1. The control for VSC on rotor side (VSCR) is achieved by considering the wind speed fluctuations for smooth connection of DG stator to the DFIG-solar-BES based isolated microgrid.
2. An additional frequency loop is incorporated in the VSCR control for minimizing the fluctuations in wind power. Moreover, the control logic to generate the synchronizing signal for static transfer switch (STS) is presented.
3. The VSCR control is designed to harness peak wind power. Moreover, the control aims to build the rated voltage at the stator of DFIG.
4. The VSCL control is designed to regulate the DG output for optimal fuel operation once STS is ON, along with power quality aspects.
5. The microgrid is designed with minimum number of power converters as compared with conventional configuration. Therefore, the overall cost of the system is reduced.

6. The microgrid is formed with renewable like wind and solar along with DG and a battery, thereby, it improves the overall system reliability with reduced intermittency.
7. Simulated performance is studied for constant and varying wind speeds, variable insolation's and at unbalanced connected loads to demonstrate the system performance.
8. Test results are demonstrated at different operating conditions to evidence the practicality of isolated microgrid for remote area applications.

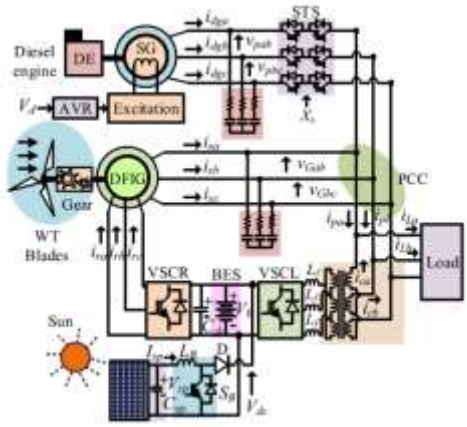


Fig 1: Isolated micro grid with WT driven DFIG, and solar-diesel-battery energy storage system

3. Microgrid configuration

The wind turbine driven DFIG, solar PV array, DG and battery based isolated microgrid, is depicted in Fig. The DFIG stator is connected to the PCC and the DG is connected to PCC through STS. The DG consists of a synchronous generator with the speed governor and an automatic voltage regulator (AVR). The AVR regulates the terminal voltage of DG as per the input voltage (*Vd*) command. The DFIG has VSCR and VSCL with common DC link along with the battery. The solar PV array is connected at the DC link through a boost converter (BC). An incremental conductance based solar MPPT [26], is used to generate the duty cycle for BC. Ripple filters are used on both sides of STS
to remove the switching ripples in voltages. Moreover, the loads are connected on Y-side of Δ/Y transformer. Various current and voltage signals used for control of microgrid, are depicted in Fig. 1. Different components of microgrid are designed as per the literature reported in [11]. The control algorithms of VSCs, are discussed in the following section.

Control algorithms of VSCS

The microgrid contains VSCR and VSCL to control the various parameters. Therefore, it necessitates one unique control for each converter. Moreover, the STS requires control signal for its smooth operation. The control of VSCR and VSCL, are discussed as follows.

Synchronizing Control of VSCR With additional Frequency Loop

The synchronizing control of VSCR, is depicted in Fig. 2. It is aimed to build the rated voltage at the DFIG stator, and to acquire peak wind power along with synchronization of DG to DFIG-solar-BES system. The DG is used to meet the base load demand by operating in optimal fuel mode whenever generation is reduced and BES is unable to discharge. Whenever, the rotor speed (ωg) and wind speed (Vw) cross its minimum allowable values ($\omega g1$, $Vw1$), the AND logic gives the signal, *XR*. The manual control switch (MS1) is provided with two inputs i.e., *XR* and logic (0/1), which is controlled manually with control signal *Mc*. The control signal of MS1 (*Mc*) is either logic 0 or 1. If *Mc* is 1 then the signal to VSCR, *XVSC_R* is equal to *XR* otherwise it is controlled manually. Based on*Mc* the turn ON/OFF of VSCR is performed. Once VSCR is ON, it starts building the voltage at the DFIG stator by generating the d-axis reference component of rotor current ($i* rd$). It is to be noted that VSCR is operated in field oriented control approach. Moreover, the synchronizing signal (*Xs*) to STS is generated by comparing the voltages, frequencies and phase angles between PCC and DG. If the phase voltage at PCC (*VrG*) is within the minimum and maximum limits of phase voltage at DG stator (*Vrpmn*, *Vrpmx*) then AND operator gives logic '1'. Similarly, frequency and phase angle error, are checked to generate the signal *Xs*, as depicted in Fig. 2. The θp, θG, θer, $\theta ermn$, $\theta ermx$, *fG*, *fpmn*, *fpmx*, denote the phase angle of DG voltage, PCC voltage phase angle, phase angle error, minimum and maximum phase error, DFIG stator frequency and, minimum and maximum frequency limits at DG side, respectively. When *XVSC_R* = 1, then $i* rd$ is generated from the PCC phase voltage reference ($V* rG$) and its actual values ($V* rG$, *VrG*) comparison and passing error through PI controller (*PIV*). The

computation of θsl is clearly depicted in the control of VSCL in the subsequent subsection. Furthermore, it is noted that the pulses are generated to VSCR only when the status signal, *XVSC_R* is logic 1 otherwise VSCR remains non-operational

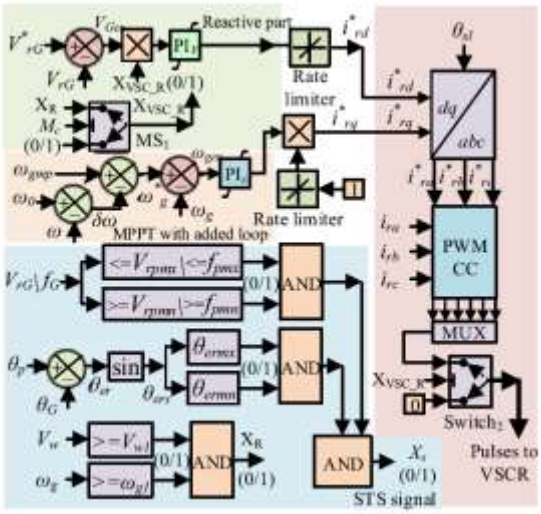


Fig 2: Synchronizing control of VSCR with additional frequency loop

B. Control of VSCL

The control of VSCL is depicted in Fig. 3 and it is developed with voltage orientation. It is aimed to regulate the DG power and to achieve the power quality aspects such as unbalanced compensation of loads etc. It also assists in maintaining the balanced and sinusoidal system currents and voltages. As shown in Fig,

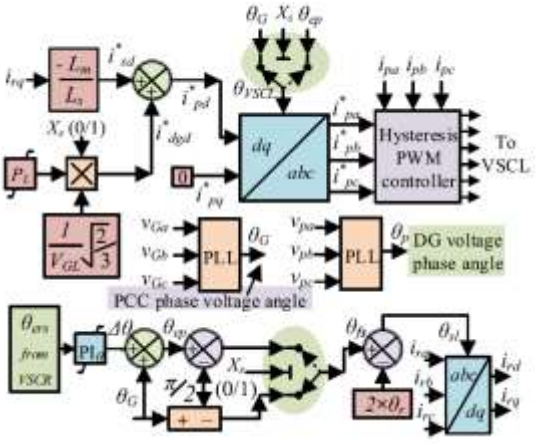


Fig 3: VSCL control

4. Fuzzy Logic controller

Fuzzy Logic is a multi-esteemed logic which is like human speculation and elucidation. It has the capability of consolidating human heuristics into PC helped basic leadership. Fuzzy logic controller (FLC) is made of fuzzification; learning and inference unit and defuzzification are demonstrated in Fig.1. The fuzzy logic needs that variable utilized as a part of depicting the control rules ought to be communicated as far as fuzzy set variables with linguistic names. Behind the guidelines have been assessed, the final gait to finish the calculation is to figure the fresh result of the fuzzy calculation by means of defuzzification.

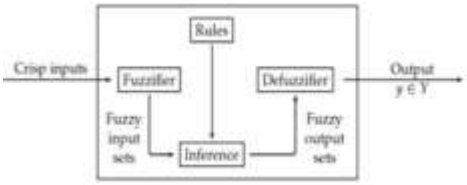


Fig 4: Fuzzy logic structure

The primary favorable position of FLC is that Fuzzy Logic portrays frameworks regarding a mix of numerics and etymology (symbolics). This has points of interest over immaculate scientific (numerical) approaches or unadulterated typical methodologies in light of the fact that all the time framework information is accessible in such a mix and furthermore fuzzy logic some of the time utilizes just

5. Simulation diagram and results

Proposed simulation model

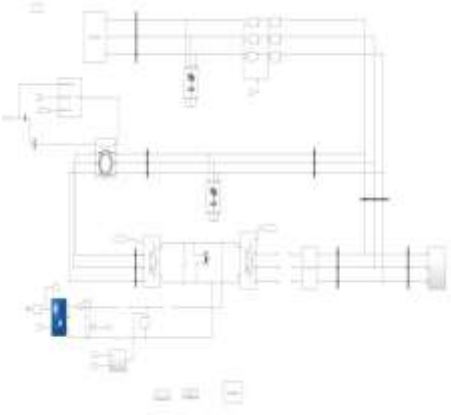


Fig 5: Proposed system model

Simulation results

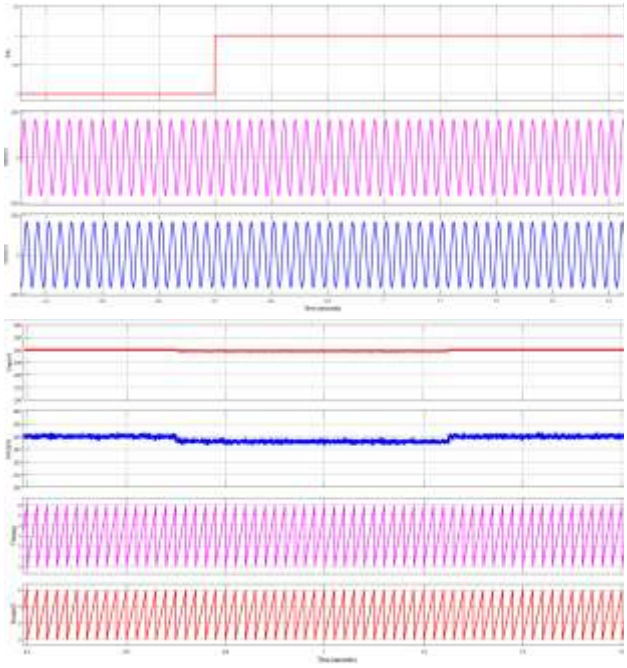
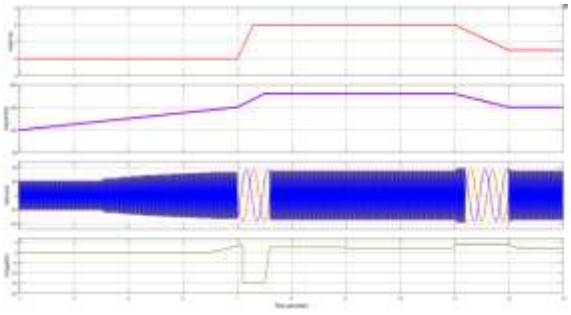


Fig 6: System performance during synchronization of DG to DFIG-solar-BES based isolated micro grid.

Fig. 6 depicts the performance of system during synchronization of DG to DFIG-solar-battery based isolated micro grid. It is noted that the DGis connected to the system when the generation is lower and the battery is unable to meet the local load. Fig. 5 illustrates the waveforms of *Xs*, *vpa*, *vGa*, *Vrp*, *VrG*, θp and θG. From these results, it is apparent that as soon as *vGa* matches with *vpa*, *VrG* matches with *Vrp*, phase error between θp and θG



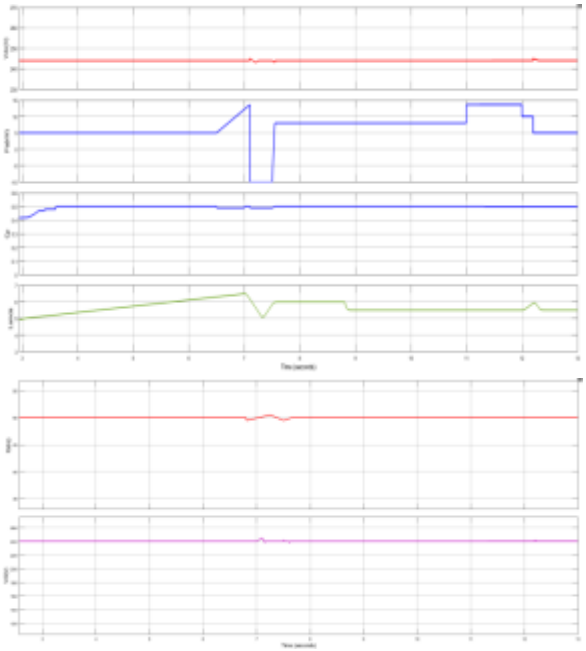


Fig 7: System performance at variable wind speeds

Fig. 7 depicts the waveforms of *Vw*, ωg, *irabc*, *Pdg*, *Vdc*, *Ps*, *Cp*, λ, *fG*.and *VrG*. *Vw* is varied from 6 m/s to 8 m/s and again it is reduced to 6.5 m/s. It is found that *Pdg* is zero before STS is ON and starts flowing after STS is ON. The frequency variation of rotor currents is evident from *irabc* waveforms. It is noted that the frequency of rotor currents is decreased to nearly zero close to the synchronous speed region of DFIG. However, *Cp* and λ are regulated to operate at wind MPPT. Moreover, PCC voltage and frequency are maintained at constant values. The variation of reference and actual rotor speeds with change in *Vw* is depicted in Fig. 6. It is noted that the *Vw* is decreased from 8 m/s to 6.5 m/s in a very short span of time. Therefore, due to the inertia of machine, the stator power exceeds its rating after t = 11 s for short time. However, at steady state *Ps* reaches its normal value as per the wind speed.

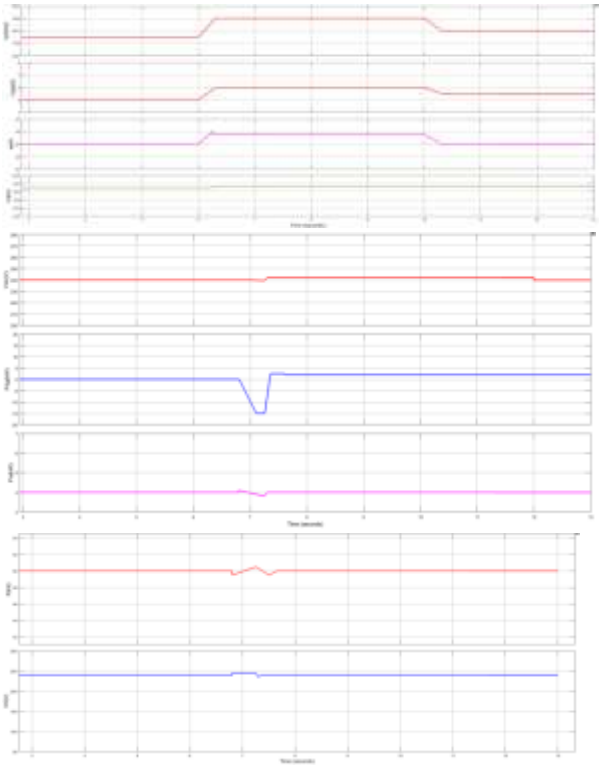
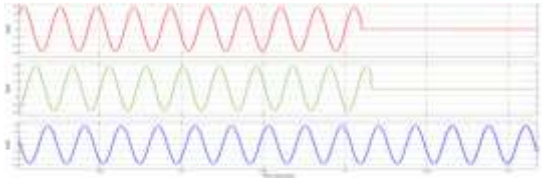
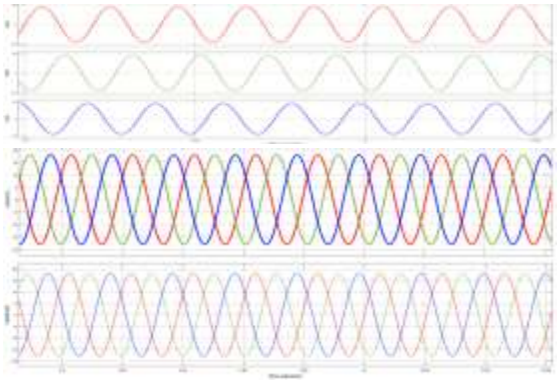


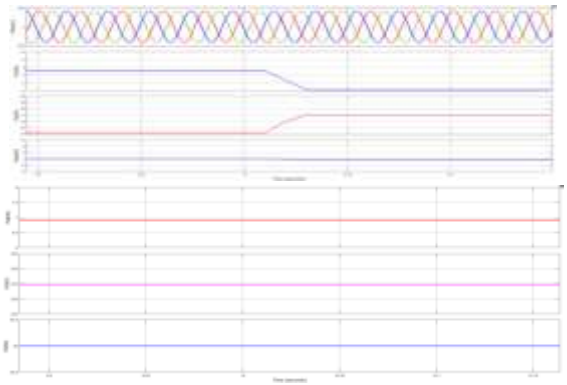
Fig 8: System performance at varying solar PV insulation

Fig. 8 depicts the system response at change in solar insolation from 750 W/m2 to 900 W/m2 and it is reduced again to 800 W/m2. Fig. 8demonstrates the waveforms of *G*, *Psp*, *Isp*, *Vsp*, *Vdc*, *Pdg*, *Ps*, *fG*.and *VrG*. From these results, it is apparent that *Psp*, *Isp* and *Vsp* are changed with insolation, which shows the solar MPPT. However, the DFIG power remains constant as wind speed is kept constant. The frequency and voltage at PCC, are regulated. The DC link voltage is varied between its allowable range, as the battery is connected. The BES charges and discharges based on generation-demand profile. Moreover, the DG supplies the power when STS is ON which is evident from Fig. 8.





(a)



(b)

Fig 9: (a,b) System performance at unbalanced connected load with optimal fuel operation of DG.

Fig. 9(a), (b) illustrate the system response at unbalanced loads. Fig. 8(a) demonstrates the waveforms of *iLa*, *iLb*, *iLc*, *ica*, *icb*, *icc*, *isabc* and *idgabc* and Fig. 8(b) depicts the waveforms of *vpabc*, *PL*, *Pc*, *Pdg*, *Ps*, *Vrp* and *fp*. The phase-a and phase-b of load, are disconnected just after t = 10 s. This creates the unbalance in the connected load and moreover, the load power is reduced as shown in Fig. 8(b). The decreased load power flows to the BES through VSCL because the DG, DFIG stator and PV powers are constant. Therefore, the *Pc* is increased when the load is disconnected. Moreover, the VSCL currents, *ica* and *icb*, are increased just after load removal because of compensation of unbalanced load and increased flow of current to BES through VSCL. It is noted that the DG power is regulated even at unbalanced loads. Furthermore, *Vrp* and *fp* are

maintained at 240 V and 50 Hz, respectively. Moreover, DFIG stator and DG currents, and voltages, are maintained balanced and sinusoidal with optimal fuel operation of DG. It shows the effectiveness of VSCL control.

Extension with fuzzy logic controller

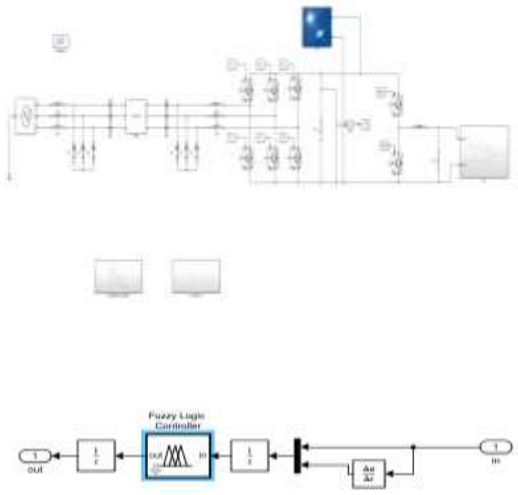


Fig 10: Fuzzy logic controller

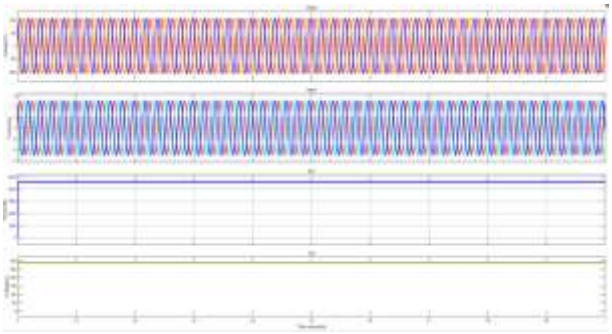


Fig 11: System performance at varying solar PV insolation

Fig. 11 demonstrates the waveforms of *G*, *Psp*, *Isp*, *Vsp*, *Vdc*, *Pdg*, *Ps*, *fG*.and *VrG*. From these results, it is apparent that *Psp*, *Isp* and *Vsp* are changed with insolation using fuzzy logic controller, which shows the solar MPPT. However, the DFIG power remains constant as wind speed is kept constant. The frequency and voltage at PCC, are regulated. The DC link voltage is varied between its allowable range, as the battery is connected. The BES charges and discharges based on generation-demand profile. Moreover, the DG supplies the power when STS is ON which is evident from Fig. 11.

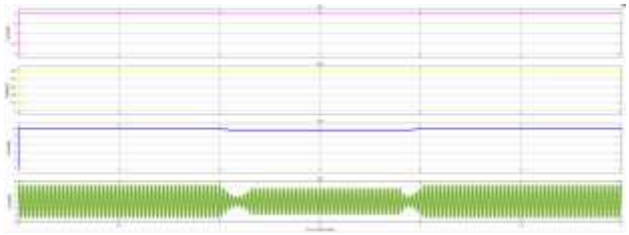


Fig 12: (a-b) System performance at unbalanced connected load with optimal fuel operation of DG

Fig. 12(a) demonstrates the waveforms of *iLa*, *iLb*, *iLc*, *ica*, *icb*, *icc*, *isabc* and *idgabc* and Fig. 8(b) depicts the waveforms of *vpabc*, *PL*, *Pc*, *Pdg*, *Ps*, *Vrp* and *fp*. The phase-a and phase-b of load, are disconnected just after t = 10 s. This creates the unbalance in the connected load and moreover, the load power is reduced as shown in Fig. 12(b). The decreased load power flows to the BES through VSCL because the DG, DFIG stator and PV powers are constant. Therefore, the *Pc* is increased when the load is disconnected. Moreover, the VSCL currents, *ica* and *icb*, are increased just after load removal because of compensation of unbalanced load and increased flow of current to BES through VSCL. It is noted that the DG power is regulated even at unbalanced loads. Furthermore, *Vrp* and *fp* are maintained at 240 V and 50 Hz, respectively. Moreover, DFIG stator and DG currents, and voltages, are maintained balanced and sinusoidal with optimal fuel operation of DG. It shows the effectiveness of VSCL control.

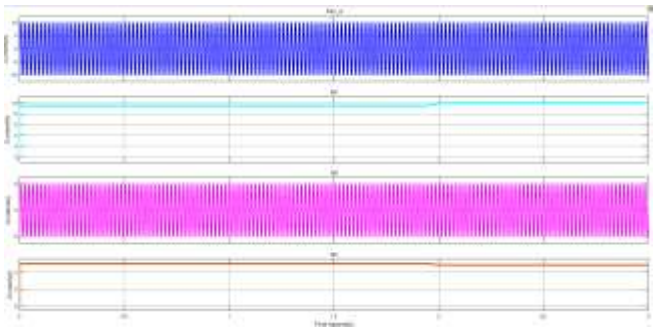


Fig 13: System currents

6. Conclusion

The synchronizing control has been presented for smooth connection of DFIG system to the DG in an isolated microgrid involving the solar PV array and the battery. The wind variations have been taken in to account for successful operation of rotor side VSC along with additional frequency loop. Effective generation of voltage at the DFIG stator has been found when VSCR is ON. Moreover, the ON status of VSCR is found when the rotor speed crosses its minimum allowable range. Moreover, the wind MPPT is obtained. In addition, it is found that STS is ON only when the frequency, voltage and phase angle of the DFIG stator/PCC match with that of DG. Furthermore, the load side VSC control has been effective in achieving the optimal fuel operation of DG even at unbalanced loads. Since the microgrid is designed with more power sources, it delivers reliable power to the connected loads with reduced intermittency. Moreover, the system is cost effective as it is configured with minimum power converters. Satisfactory performance of isolated microgrid has been found at simulated scenarios such as synchronization of DG to the DFIG-solar-battery based isolated microgrid at steady, varying wind speeds, varying solar PV insolations and at unbalanced connected loads. Moreover, experimental results at varying winds, varying PV insolation, change in load and during DG connection/disconnection have proven the practicality and robustness of isolated microgrid. Furthermore, the microgrid voltages and currents are appeared balanced and sinusoidal, and their THDs are found within the acceptable limits of IEEE 519 standard.

References

[1] R. K. Sharma, S. Mudaliyar, and S. Mishra, "A DC droop-based optimal dispatch control and power management of hybrid photovoltaic-battery and diesel generator standalone AC/DC system," *IEEE Syst. J.*, vol. 15, no. 2, pp. 3012–3023, Jun. 2021.

[2] A. R. Nair, R. Bhattarai, M. Smith, and S. Kamalasadan, "Parametrically robust identification based sensorless control approach for doubly fed induction generator," *IEEE Trans. Ind. Appl.*, vol. 57, no. 1, pp. 1024–1034, Jan./Feb. 2021.

[3] B.Hu, H. Nian,M. Li,Y. Xu,Y. Liao, and J.Yang, "Impedance-based analysis and stability improvement of DFIG system within PLL bandwidth," *IEEE Trans. Ind. Electron.*, vol. 69, no. 6, pp. 5803–5814, Jun. 2022.

[4] A. S. A. Awad, D. Turcotte, and T. H. M. El-Fouly, "Impact assessment and mitigation techniques for high penetration levels of renewable energy sources in distribution networks: Voltage-control perspective," *J. Modern Power Syst. Clean Energy*, vol. 10, no. 2, pp. 450–458, Mar. 2022.

[5] J. Huang, Z. Yang, J. Yu, J. Liu, Y. Xu, and X. Wang, "Optimization for DFIG fast frequency responsewith small-signal stability constraint," *IEEE Trans. Energy Convers.*, vol. 36, no. 3, pp. 2452–2462, Sep. 2021.

[6] B. Bossoufi et al., "Rooted tree optimization for the backstepping power control of a doubly fed induction generator wind turbine: DSPACE implementation," *IEEE Access*, vol. 9, pp. 26512–26522, 2021.

[7] A. T. Nguyen and D.-C. Lee, "Sensorless control of DFIG wind turbine systems based on SOGI and rotor position correction," *IEEE Trans. Power Electron.*, vol. 36, no. 5, pp. 5486–5495, May 2021.

[8] P. K. Gayen, "Stator flux producing current based promoted rotor angle estimator of doubly-fed induction generator for encoderless operations," *IEEE Sensors J.*, vol. 21, no. 13, pp. 15133–15141, Jul. 2021.

[9] X. Lyu, Y. Jia, and Z. Dong, "Adaptive frequency responsive control for wind farm considering wake interaction," *J. Modern Power Syst. Clean Energy*, vol. 9, no. 5, pp. 1066–1075, Sep. 2021.

[10] Y. Mi, Y. Song, Y. Fu, and C. Wang, "The adaptive sliding mode reactive power control strategy for wind–diesel power system based on sliding mode observer," *IEEE Trans. Sustain. Energy*, vol. 11, no. 4, pp. 2241–2251, Oct. 2020.

[11] S. K. Tiwari, B. Singh, and P. K. Goel, "Control of wind–diesel hybrid system with BESS for optimal operation," *IEEE Trans. Ind. Appl.*, vol. 55, no. 2, pp. 1863–1872, Mar./Apr. 2019.

[12] Y. Zhang, T. Jiang, and J. Jiao, "Model-free predictive current control of a DFIG using an ultra-local model for grid synchronization and power regulation," *IEEE Trans. Energy Convers.*, vol. 35, no. 4, pp. 2269–2280, Dec. 2020.

[13] D. Vijay M, G. Bhuvaneswari, and B. Singh, "A reliable microgrid comprising solar PV-WEGS and battery with seamless power transfer capability," *IEEE Trans. Ind. Electron.*, vol. 68, no. 10, pp. 9665–9674, Oct. 2021.

[14] R. Rosso, X. Wang, M. Liserre, X. Lu, and S. Engelken, "Grid-forming converters: Control approaches, grid-synchronization, and future trends— A review," *IEEE Open J. Ind. Appl.*, vol. 2, pp. 93–109, 2021.

[15] S. Puchalapalli and B. Singh, "Control of seamless transition between islanding and grid connected modes in WT driven doubly fed induction generator-based microgrid," in *Proc . IEEE Int. Conf. Sustain. Energy Future Electric Transp.*, 2021, pp. 1–6.

[16] Y. Mi et al., "Robust load frequency control for isolated microgrid based on double-loop compensation," *CSEE J. Power Energy Syst.*, early access, Dec. 30, 2021, doi: 10.17775/CSEEJPES.2020.04800.

[17] S. Morovati, Y. Zhang, S. M. Djouadi, K. Tomsovic, A. Wintenberg, and M. Olama, "Robust output feedback control design for inertia emulation by wind turbine generators," *IEEE Trans. Power Syst.*, vol. 36, no. 6, pp. 5056–5067, Nov. 2021.

[18] N. Mendis, K. M. Muttaqi, S. Perera, and S. Kamalasadan, "An effective power management strategy for a wind–diesel–hydrogen-based remote area power supply system to meet fluctuating demands under generation uncertainty," *IEEE Trans. Ind. Appl.*, vol. 51, no. 2, pp. 1228–1238, Mar./Apr. 2015.

[19] F. Dubuisson, M. Rezkallah, A. Chandra, M. Saad, M. Tremblay, and H. Ibrahim, "Control of hybrid wind–diesel standalone microgrid for water treatment system application," *IEEE Trans. Ind. Appl.*, vol. 55, no. 6, pp. 6499–6507, Nov./Dec. 2019.

[20] A. E. Khalil,T. A. Boghdady,M.H.Alham, and D. K. Ibrahim, "Enhancing the conventional controllers for load frequency control of isolated microgrids using proposed multi-objective formulation via artificial rabbits optimization algorithm," *IEEE Access*, vol. 11, pp. 3472–3493, 2023.

[21] M. E. Sallam, M. A. Attia, A. Y. Abdelaziz, M. A. Sameh, and A. H. Yakout, "Optimal sizing of different energy sources in an isolated hybrid microgrid using turbulent flowwater-based optimization algorithm," *IEEE Access*, vol. 10, pp. 61922–61936, 2022.

[22] A. Mohammad-Alikhani, A. Mahmoudi, R. Khezri, and S. Kahourzade, "Multiobjective optimization of system configuration and component capacity in an AC minigrid hybrid power system," *IEEE Trans. Ind. Appl.*, vol. 58, no. 3, pp. 4158–4170, May/Jun. 2022.

[23] M. Shojaee and S. M. Azizi, "Decentralized robust control of a coupled wind turbine and diesel engine generator system," *IEEE Trans. Power Syst.*, vol. 38, no. 1, pp. 807–817, Jan. 2023.

[24] H. Minor-Popocatl, O. Aguilar-Mejía, F. D. Santillán-Lemus, A. Valderrabano-Gonzalez, and R.-I. Samper-Torres, "Economic dispatch in micro-grids with alternative energy sources and batteries," *IEEE Latin Amer. Trans.*, vol. 21, no. 1, pp. 124–132, Jan. 2023.

[25] H. M. Fekry, A. A. Eldesouky, A. M. Kassem, andA.Y.Abdelaziz, "Power management strategy based on adaptive neuro fuzzy inference system for AC microgrid," *IEEE Access*, vol. 8, pp. 192087–192100, 2020.

[26] X. Li, H. Wen, Y. Hu, Y. Du, and Y. Yang, "A comparative study on photovoltaic MPPT algorithms under EN50530 dynamic test procedure," *IEEE Trans. Power Electron.*, vol. 36, no. 4, pp. 4153–4168, Apr. 2021